Записки научных
семинаров ПОМИ
Том 548, 2025 г.

F. Colomo, M. Mannatzu, A. G. Pronko

THE FIVE-VERTEX MODEL AS A DISCRETE LOG-GAS

Abstract. We consider the five-vertex model on a rectangular domain of the square lattice, with the so-called "scalar-product" boundary conditions. We address the evaluation of the free-energy density of the model in the scaling limit, that is when the number of sites is sent to infinity and the mesh of the lattice to zero, while keeping the size of the domain constant. To this aim, we reformulate the partition function of the model in terms of a discrete log-gas, and study its behaviour in the thermodynamic limit. We reproduce previous results, obtained by using a differential equation approach. Moreover, we provide the explicit form of the resolvent in all possible regimes. This work is preliminary to further studies of limit shape phenomena in the model.

Dedicated to Nikolai Mikhailovich Bogoliubov on the occasion of his 75th birthday

1. Introduction

The five-vertex model is a particular case of the six-vertex model, with one of its Boltzmann weights set equal to zero [1, 2]. Historically, it was first introduced as a model of crystal growth and melting, basing on the terrace-ledge-kink picture of a crystal surface [3]. Its exact solution and phase diagram, in the case of periodic boundary conditions, were worked out in [4]. The model was further studied in connection with interacting domain walls [5], and as an interacting generalization of dimer coverings of the honeycomb lattice [6]. Recent interest in the five-vertex model is also based, among others, on its relation with symmetric functions [7–10].

Our main motivation for studying the five-vertex model stems from the fact that, under specific choices of fixed boundary conditions, and just as its ascendent, the six-vertex model, it exhibits phase separation and limit shape phenomena. In recent times, relevant progresses have been achieved

Key words and phrases: Scalar product boundary conditions, Hankel determinants, matrix models, third-order phase transition, plane partitions.

towards an understanding of the scaling properties of the five-vertex model in a rather general setup, by variational methods [11–14].

Here we are interested specifically in the case of "scalar-product", or "boxed-plane-partition", boundary conditions [15–20], where explicit determinantal expressions of Hankel type are known for the partition function [21, 22], and for the boundary correlation function [23]. These Hankel determinant representations correspond to analogous ones obtained for the six-vertex model with domain wall boundary conditions [24–26]. They turn out to be especially convenient, in view of the various available techniques to study their asymptotic behaviour in the scaling limit. In particular, explicit knowledge of the asymptotic behaviour of the boundary correlation function would allow for the derivation, via the "tangent method" [27], of the expression of the phase separation, or arctic curve, of the model.

In the case of the partition function of the model, its asymptotic expansion for large lattice sizes has been worked out in [28]. The derivation is based on the fact that one of the determinant representations appears to be the τ-function of the Painlevé VI. It uses an approach originally proposed in [29], based on the corresponding σ-form of the Painlevé VI [30, 31]. The method is very efficient and systematic, however it is unclear how it can be applied to the boundary correlation functions.

An alternative method, inspired by [32], where it was applied to the case of the six-vertex model, is based on random matrix model techniques. Although less powerful in evaluating subleading corrections, this method appears to be more suitable for direct extension to "modified" Hankel determinants such as those appearing in expressions for boundary correlation function (see, e.g., [33], for the case of the domain-wall six-vertex model).

Our goal here is therefore to work out the exact expression, in the scaling limit, of the free-energy density of the five-vertex model with scalar-product boundary conditions, basing on a discrete log-gas description, and on random matrix model techniques [34]. We reproduce, at the leading order, the expressions first derived in [28]. On the other hand, we evaluate the explicit form of the resolvent in the various regimes of the considered log-gas. This is a propaedeutic result to the evaluation of the asymptotic behaviour of the boundary correlation function, and, via the "tangent method", of the arctic curve of the model. These two problems will be addressed elsewhere.

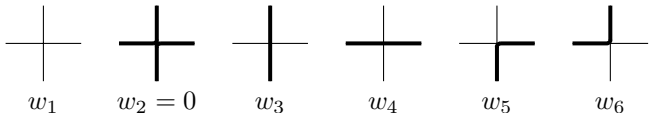

Fig. 1. The six vertex configurations of the six-vertex model, represented in terms of lines, and their Boltzmann weights in the five-vertex model.

We organize the paper as follows. In the next Section we review the five-vertex model with scalar-product boundary conditions and recall various relevant results. In Section 3 we reformulate the partition function of the model in terms of a discrete log-gas, and show how to use the resolvent technique for the evaluation of the free-energy density. The two cases where the asymptotic form of the domain is a square or a rectangle must be considered separately. They are treated in detail in Section 4 and 5, respectively. Results and perspectives are discussed in Section 6. Some technical aspects of the derivation are given in three Appendices.

2. The five-vertex model

2.1. The model. We consider the five-vertex model on an $L \times M$ lattice (i.e., built from the intersection of L vertical and M horizontal lines), with a special choice of fixed boundary conditions, so-called "scalar-product", or "boxed-plane-partition", boundary conditions [15–20].

The five-vertex model is a particular case of the six-vertex model, with one of its Boltzmann weights set equal to zero. The configurations of the model can be represented in terms of arrows, or equivalently, in terms of thick or thin (or empty) edges, with the thick edges describing paths flowing through the lattice. We will use this last representation, with the conventions of Fig. 1.

The Boltzmann weights may be parameterized as follows:

$$w_1 = \frac{\alpha}{\Delta}\frac{x-1}{\sqrt{x}}, \quad w_3 = \frac{\sqrt{x}}{\alpha}, \qquad w_4 = \alpha\sqrt{x}, \quad w_5 = w_6 = 1.$$

The parameter $\alpha \geqslant 0$ may be interpreted in terms of an external vertical electric field. In the quantum inverse scattering method formalism [15, 22] the parameters $x > 0$ and $\Delta \in \mathbb{R}$ may be viewed as (the square of) a spectral parameter and as a crossing parameter, respectively. We have

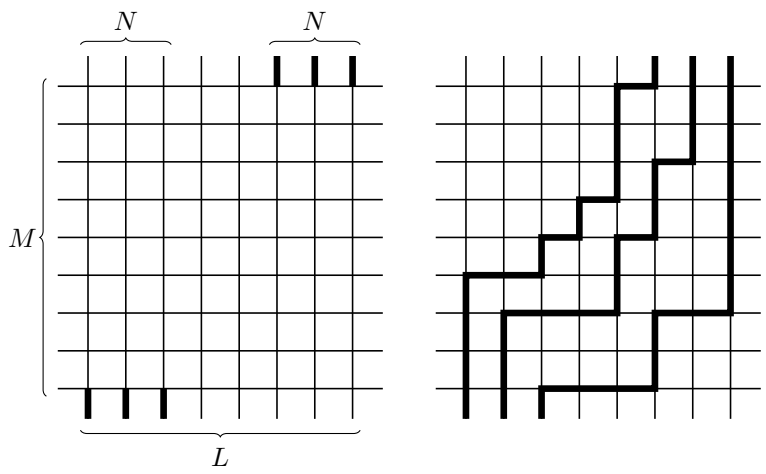

Fig. 2. The $L \times M$ lattice, with scalar-product boundary condition (left), and a possible configuration of the model (right). Here $L = 8$, $M = 9$, and $N = 3$.

$x \in (0, 1)$ for $\Delta < 0$, and $x \in (1, \infty)$ for $\Delta > 0$. The parameter Δ may be defined independently of the parametrization, as follows:

$$\Delta = \frac{w_3 w_4 - w_5 w_6}{w_1 w_3}.$$

The free-fermion point of the model may be obtained, e.g., by letting $x = \mathrm{e}^{\Delta v}$ and sending $\Delta \to 0$.

The scalar-product boundary conditions correspond to fixing N paths entering vertically from the N rightmost top boundary edges, and exiting vertically from the N leftmost bottom boundary edges, see Fig. 2. Interestingly, the configurations of the five-vertex model with scalar-product boundary conditions, with N lines on the $L \times M$ lattice, are in bijection with the boxed plane partitions fitting in an $(L-N) \times N \times (M-N)$ box [17,21]. In the correspondence, the paths of the five-vertex model are simply the "gradient lines" of the surface of the boxed plane partition.

The partition function $Z = Z_{N,M,L}(x; \Delta, \alpha)$, is defined in the standard way,

$$Z = \sum_{\mathcal{C}} \prod_{i=1,3,4,5,6} w_i^{n_i(\mathcal{C})},$$

where the sum is taken over all admissible configurations $\mathcal{C}$, and $n_i(\mathcal{C})$ is the number of vertices of type i in configuration $\mathcal{C}$.

Note that when the model is considered with the scalar-product boundary conditions, each admissible configuration $\mathcal{C}$ has the following properties:

- $n_1(\mathcal{C}) = (L-N)(M-N)$;
- vertices of type 3 and 4 always appear in pairs, with $n_3(\mathcal{C}) - n_4(\mathcal{C}) = N(N+M-L)$;
- $n_5(\mathcal{C}) = n_6(\mathcal{C})$.

It follows from these conditions that the Boltzmann weight of any given configuration $\mathcal{C}$ will be of the form

$$w(\mathcal{C}) = \left(\frac{\alpha}{\Delta}\frac{x-1}{\sqrt{x}}\right)^{(L-N)(M-N)} \alpha^{-N(M+N-L)} x^{[n_3(\mathcal{C})+n_4(\mathcal{C})]/2}.$$

There are exactly $\binom{M}{N}$ configurations with maximal number of vertices of type 3 and 4, and correspondingly, minimal number of vertices of type 5 and 6 (with $n_5 = n_6 = N$). All these configurations have Boltzmann weight

$$E_{N,M,L}(x;\Delta,\alpha) = \left(\frac{x-1}{\Delta}\right)^{(L-N)(M-N)} \left(\frac{\alpha}{\sqrt{x}}\right)^{M(L-2N)} x^{N(L-N-1)}.$$

We may thus write the partition function as

$$Z = \binom{M}{N} E_{N,M,L}(x;\Delta,\alpha) P_{N,M,L}(x^{-1}), \tag{2.1}$$

where $P_{N,M,L}(x^{-1})$ is a polynomial in x^{-1}, satisfying the normalization condition

$$P_{N,M,L}(0) = 1. \tag{2.2}$$

The polynomial $P_{N,M,L}(x^{-1})$ is of degree equal to the difference between the maximal and minimal number of pairs of vertices of type 5 and 6:

$$\deg P_{N,M,L}(x^{-1}) = N \min(M-N, L-N-1). \tag{2.3}$$

The polynomial $P_{N,M,L}(x^{-1})$ is symmetric under the interchange $L \leftrightarrow M+1$,

$$P_{N,M,L}(x^{-1}) = P_{N,L-1,M+1}(x^{-1}),$$

however the partition function Z is not. We have no simple explanation for this symmetry at the moment, but it is indeed evident from the Hankel determinant representation given below.

2.2. Particular cases. We report here on some particular cases which may be evaluated explicitly in closed form, see [28]. These results will turn out useful below.

Let us first consider the model at its free-fermion point, by letting $x = \mathrm{e}^{\Delta v}$, and sending $\Delta \to 0$. When the parameters v and α are furthermore set to 1, all weights become equals to 1. Recalling that the configurations of the five-vertex model are in bijection with boxed plane partitions [17, 21], we simply have

$$\lim_{\Delta\to 0} Z_{N,M,L}(\mathrm{e}^{\Delta}; \Delta, 1) = \mathrm{PL}(L-N, N, M-N),$$

where

$$\mathrm{PL}(a,b,c) = \prod_{j=1}^{a} \frac{(b+c+j-1)!(j-1)!}{(b+j-1)!(c+j-1)!} \tag{2.4}$$

is the celebrated MacMahon's formula for the number of boxed plane partitions in a box of size $a \times b \times c$. It is easy to check that in the considered limit, $E_{N,M,L}(\mathrm{e}^{\Delta v}; \Delta, 1) \to 1$, and thus, from (2.1),

$$P_{N,M,L}(1) = \binom{M}{N}^{-1} \mathrm{PL}(L-N, N, M-N). \tag{2.5}$$

By using MacMahon's formula (2.4), one may check that $P_{N,M,L}(1)$ is symmetric under the interchange $L \leftrightarrow M+1$.

Also, letting $x = \alpha^2$ and $\Delta = -1$ in the Boltzmann weights of the five-vertex model, in the limit $\alpha \to 0$ one recovers the four-vertex model, whose configurations are again in bijection with boxed plane partitions (although of different sizes), provided that $M \geqslant L-1$, see [16, 35]:

$$\lim_{\alpha\to 0} Z(\alpha^2; -1, \alpha) = \mathrm{PL}(N, M-L+1, L-N), \qquad M \geqslant L-1.$$

This observation allows us to evaluate the leading term of the polynomial $P_{N,M,L}(x^{-1})$ in the case $L \leqslant M+1$ (see also (2.3)):

$$\lim_{x\to 0} x^{N(L-N-1)} P_{N,M,L}(x^{-1}) = \binom{M}{N}^{-1} \mathrm{PL}(N, M-L+1, L-N), \qquad L \leqslant M+1. \tag{2.6}$$

Note that, when setting $L = M$, the RHS simplifies to 1. Indeed, when $L = M$, there is only one configuration maximizing the number of vertices of type 5 and 6. According to [28], in the complementary case $L \geqslant M+1$

one has

$$\lim_{x\to 0} x^{N(M-N)} P_{N,M,L}(x^{-1}) = \binom{L-1}{N}^{-1} \mathrm{PL}(N, L-M-1, M-N+1), \quad L \geqslant M+1. \tag{2.7}$$

It may be easily checked that indeed the last two expressions are related through the interchange $L \leftrightarrow M+1$.

2.3. Hankel determinant representation. Various determinant representations has been worked out for the partition function of the model [22, 28]. Here we shall resort to the following one:

$$P_{N,M,L}(x^{-1}) = x^{N(N-1)/2}\, \tau_{N,M,L}(x^{-1}),$$

with

$$\tau_{N,M,L}(x^{-1}) = N!\, C_{N,M,L} \times \det_{1\leqslant i,j,\leqslant N} \left[(x\partial_x)^{i+j-2}\, {}_2F_1 \left(\begin{matrix} -L+2, -M+1 \\ 2 \end{matrix} \middle| \frac{1}{x} \right) \right], \tag{2.8}$$

and

$$C_{N,M,L} = \prod_{j=0}^{N-1} \frac{(L-N+j-1)!(M-N+j)!}{(L-2)!(M-1)!}. \tag{2.9}$$

This representation, of Hankel type, has been derived in [28], see Eq. (2.6) therein.

2.4. Scaling limit and free-energy density. We are interested in the evaluation of the free-energy density of the model in the scaling limit, keeping its geometry fixed. To this aim, let us introduce the two rescaled geometric parameters $\lambda, \mu \in [1, \infty)$, as follows: $L = \lfloor \lambda N \rfloor$, and $M = \lfloor \mu N \rfloor$. We are interested in the limit $N \to \infty$, with λ and μ fixed.

The free-energy density of the model is defined as

$$F := -\lim_{N\to\infty} \frac{1}{\lambda\mu N^2} \log Z_{N,\lfloor \mu N \rfloor, \lfloor \lambda N \rfloor}.$$

It is given by

$$F = -\frac{f_2(x)}{\mu\lambda} - \frac{(\mu-1)(\lambda-1)}{\mu\lambda} \log \frac{x-1}{\Delta} + \frac{\mu\lambda - 2}{2\mu\lambda} \log x - \frac{\lambda-2}{\lambda} \log \alpha,$$

where the function

$$f_2(x) := \lim_{N\to\infty} \frac{1}{N^2} \log P_{N,\lfloor \mu N\rfloor,\lfloor \lambda N\rfloor}(x^{-1}) \tag{2.10}$$

describes the leading behaviour of the nontrivial factor $P_{N,M,L}(x^{-1})$ in the partition function, see (2.1).

As a consequence of the normalization condition (2.2) the quantity $f_2(x)$ satisfies

$$\lim_{x\to\infty} f_2(x) = 0. \tag{2.11}$$

Relation (2.5) implies

$$f_2(1) = \Psi(\lambda-1, \mu-1), \tag{2.12}$$

where the function $\Psi(a,b)$ is given by

$$\Psi(a,b) = \frac{1}{4}\Big[\ell\left(a^2\right) - \ell\left((a+1)^2\right) + \ell\left(b^2\right) - \ell\left((b+1)^2\right) - \ell\left((a+b)^2\right) + \ell\left((a+b+1)^2\right)\Big], \tag{2.13}$$

and $\ell(x) = x\log x$, see Appendix A for details.

As a consequence of relations (2.6) and (2.7), we also have

$$\begin{aligned} &\lim_{x\to 0}\left[f_2(x) + (\lambda-1)\log x\right] = \Psi(\mu-\lambda, \lambda-1), \qquad \mu > \lambda, \\ &\lim_{x\to 0}\left[f_2(x) + (\mu-1)\log x\right] = \Psi(\lambda-\mu, \mu-1), \qquad \mu < \lambda. \end{aligned} \tag{2.14}$$

Note that in the case of an asymptotically square-shaped domain, $\lambda = \mu$, both conditions boil down to

$$\lim_{x\to 0}[f_2(x) + (\lambda-1)\log x] = \Psi(0, \lambda-1) = 0. \tag{2.15}$$

In particular, note that the two limits, $x \to 0$ and $N \to \infty$, do commute.

2.5. The function $\Phi(x)$. For a reason that will become apparent below, it is convenient to define the quantity

$$\Phi(x) := -\lim_{N\to\infty} \frac{1}{N^2} \log \tau_{N,\lfloor \mu N\rfloor,\lfloor \lambda N\rfloor}(x^{-1}). \tag{2.16}$$

A simple calculation shows that

$$f_2(x) := \log\sqrt{x} - \Phi(x). \tag{2.17}$$

Also, the behaviour of the function $\Phi(x)$ as $x \to 0, 1, \infty$ immediately follows from relations (2.11)–(2.12) and (2.14)–(2.15). One has

$$\Phi(1) = -\Psi(\lambda-1, \mu-1), \tag{2.18}$$

and

$$\Phi(x) = \frac{1}{2}\log x + o(x^0), \qquad x \to \infty. \tag{2.19}$$

One also has

$$\begin{aligned} \lim_{x\to 0}\left[\Phi(x) - \left(\lambda - \frac{1}{2}\right)\log x\right] &= -\Psi(\mu-\lambda, \lambda - 1), \qquad \mu > \lambda, \\ \lim_{x\to 0}\left[\Phi(x) - \left(\mu - \frac{1}{2}\right)\log x\right] &= -\Psi(\lambda-\mu, \mu - 1), \qquad \mu < \lambda. \end{aligned} \tag{2.20}$$

Note that in the case of an asymptotically square-shaped domain, $\lambda = \mu$, both conditions boil down to

$$\lim_{x\to 0}\left[\Phi(x) - \left(\lambda - \frac{1}{2}\right)\log x\right] = \Psi(0, \lambda - 1) = 0. \tag{2.21}$$

In particular, note that the two limits, $x \to 0$ and $N \to \infty$, do commute. In the following we shall focus on the evaluation of $\Phi(x)$.

3. A discrete log-gas description

3.1. The log-gas. We are interested in evaluating the function $f_2(x)$, or equivalently, the function $\Phi(x)$, describing the leading behaviour of $P_{N,M,L}(x)$ in the scaling limit. To this aim, inspired by [32], we rewrite the Hankel determinant representation (2.8) as follows:

$$\tau_{N,M,L}(x^{-1}) = C_{N,M,L} \sum_{0\leqslant k_1,\dots,k_N\leqslant m} \prod_{1\leqslant i<j\leqslant N} (k_j - k_i)^2 \prod_{i=1}^{N} \nu_{L,M}(k_i) \tag{3.1}$$

with $C_{N,M,L}$ defined in (2.9), and

$$\nu_{L,M}(k) := \binom{L-2}{k}\binom{M-1}{k}\frac{x^{-k}}{k+1}, \qquad k = 0, 1, \dots, m, \tag{3.2}$$

where $m := \min(L-2, M-1)$. In this formula one can easily recognize the discrete measure analogue of an Hermitean $m \times m$ random matrix model, namely, a discrete log-gas. To investigate its behaviour in the scaling limit, we may use standard random matrix techniques, suitably adapted to take into account the discreteness of the measure, see, e.g., [34,36] and references therein.

3.2. Scaling limit. We want to study the free-energy density of the considered log-gas in the scaling limit of large L, M, N, with fixed ratios. To this aim we rescale all parameters by N, letting $k = \lfloor Nz \rfloor$, $M - 1 = \lfloor N\mu \rfloor$, $L - 2 = \lfloor N\lambda \rfloor$, $m = \lfloor N\gamma \rfloor$. Here $\lambda, \mu > 1$, and $\gamma = \min(\lambda, \mu)$. Our model describes now a gas of particles with logarithmic interaction, confined by the continuous potential

$$V(z) := -\frac{1}{N} \lim_{N\to\infty} \log \nu_{\lfloor \mu N \rfloor, \lfloor \lambda N \rfloor}(Nz).$$

In our case, it is given by

$$V(z) = 2z \log z + (\lambda - z) \log(\lambda - z) - \lambda \log \lambda \\ + (\mu - z) \log(\mu - z) - \mu \log \mu + z \log x, \quad (3.3)$$

complemented by two hard walls, at $z = 0$, and at $z = \gamma$.

To proceed, we rely on standard results from weighted potential theory in the case of a discrete log-gas [36]. The problem may be reformulated as the evaluation of the equilibrium measure $\rho(z)$, which is the unique minimizer of the functional

$$S[\rho] = -\int \int_{z \neq w} \log|w - z| \rho(w) \rho(z) \mathrm{d}w \mathrm{d}z + \int V(z) \rho(z) \mathrm{d}z,$$

subject to the normalization condition

$$\int \rho(z) \mathrm{d}z = 1 \quad (3.4)$$

and the additional constraint

$$0 \leqslant \rho(z) \leqslant 1, \quad (3.5)$$

that follows from the discreteness of the original variables k_j [37]. In the above formulae, integration is understood over the interval $[0, \gamma]$.

As a consequence of the last constraint, the equilibrium measure partitions the interval $[0, \gamma]$ into a sequence of intervals, known as *voids*, *bands*, and *saturated regions*, according to its value: $\rho(z) = 0$, or $0 < \rho(z) < 1$, or $\rho(z) = 1$, respectively. Voids and saturated intervals go together under the name of *gaps*.

3.3. The resolvent. A convenient way to evaluate the equilibrium measure is based on the resolvent,

$$W(z) = \int_S \frac{\rho(u)}{z-u} \mathrm{d}u, \qquad z \notin S$$

where S is the support of the equilibrium measure $\rho(z)$. The resolvent has the following properties:

i) it is analytic in $\mathbb{C} \setminus S$;

ii) the normalization condition (3.4) implies the asymptotic behaviour:

$$W(z) \sim \frac{1}{z}, \qquad z \to \infty; \tag{3.6}$$

iii) the equilibrium measure and the resolvent are related by

$$\rho(z) = -\frac{1}{2\pi \mathrm{i}} \left[W(z + \mathrm{i}0) - W(z - \mathrm{i}0) \right], \qquad z \in S;$$

iv) the resolvent satisfies the "saddle-point equation":

$$W(z + \mathrm{i}0) + W(z - \mathrm{i}0) = U(z), \qquad z \in S. \tag{3.7}$$

In the case of a continuous log-gas, $U(z)$ is just equal to the derivative $V'(z)$ of the potential of the model. However, in the case of a discrete log-gas, this holds only as long as the equilibrium measure $\rho(z)$ does not saturate the constraint (3.5). The occurrence of saturation in the equilibrium measure requires modifying the form of $U(z)$ and S in (3.7), as we shall discuss later on.

Assuming that the support S consists in one single interval $[a, b]$ on the real axis, the solution of (3.7) is

$$W(z) = \frac{\sqrt{(z-a)(z-b)}}{2\pi} \int_a^b \frac{U(u)}{(z-u)\sqrt{(u-a)(b-u)}} \mathrm{d}u, \qquad z \in \mathbb{C} \setminus [a, b]. \tag{3.8}$$

Imposing that the expansion at large z of the explicit expression of the resolvent, obtained by evaluating the integral in (3.8), matches the asymptotic behaviour (3.6) provides two conditions, that determine the endpoints a and b of the support S.

3.4. The free-energy density. The free-energy density of our discrete log-gas coincides with the function $\Phi(x)$ defined in (2.16).

Denoting by E the first moment of the equilibrium measure $\rho(u)$, or equivalently, the average position of the log-gas particles, we note that it can be worked out from the asymptotic expansion of the resolvent. Indeed, one has

$$W(z) = \frac{1}{z} + \frac{E}{z^2} + O(z^{-3}), \qquad |z| \to \infty.$$

We also note that, due to the form of the potential (3.3), the free-energy density $\Phi(x)$ may be related to the first moment E by

$$x\partial_x \Phi(x) = E. \tag{3.9}$$

The log-gas free-energy density $\Phi(x)$ may thus be evaluated up to an integration constant, which may be fixed if one is able to calculate explicitly $\Phi(x)$ at some particular value of x by other means. Such calculation has indeed been done in Section 2.5, yielding conditions (2.18)-(2.21), at $x = 1$, or as $x \to 0, \infty$.

4. The case $\lambda = \mu$

As already emphasized in [28], the free-energy density of the five-vertex model exhibits different behaviours according to the asymptotic shape (square or rectangular) of the considered domain. This happens of course in the free-energy density of the corresponding log-gas as well, depending on the values of λ and μ being equal or different. The two cases must be treated separately; we start with the simplest one, where $\lambda = \mu$.

4.1. Preliminaries. When $L = M - 1$, the measure (3.2) simplifies significantly. In the scaling limit, such simplification occurs as soon as $L - M = o(N)$. In this case, the corresponding potential is similar to that associated to the orthogonalizing measure for Krawtchouk orthogonal polynomials. The asymptotic behaviour of the Krawtchouk log-gas has been studied in [38]. Note however here an overall factor 2 in the potential. As we shall see below, this yields significant differences in the asymptotic behaviour of the log-gas, with respect to the Krawtchouk case, in particular, the emergence of two third-order phase transitions in the free-energy density of the model.

In the scaling limit we have $\lambda = \mu$. The potential becomes

$$V(z) = 2[z \log z + (\lambda - z)\log(\lambda - z) - \lambda \log \lambda] + z \log x,$$

with two additional hard walls located at $z = 0$ and $z = \lambda$. The parameter $x > 0$ enters through its logarithm. When $x = 1$, the potential is symmetric under $z \leftrightarrow \lambda - z$, with its minimum at $\lambda/2$. When $x \neq 1$, the minimum of the potential, $z_m = \lambda/(\sqrt{x} + 1)$ is displaced to the right (if $0 < x < 1$) or left (if $x > 1$).

The shape of the potential, and the presence of the constraint (3.5) suggest various possible scenarios, built as suitable sequences of saturated intervals (S), bands (B), and voids (V). We shall denote each scenario by the initials of the sequence, from left to right, of these possibile behaviours of the density. Simplest scenarios have only one band. The presence of two bands would imply the necessity to solve a two-cut problem. Luckily, only one-band scenarios will occur here. More precisely, decreasing x within the interval $(0, \infty)$, three possible scenarios will emerge, namely SBV, VBV, and VBS. These three scenarios are separated by two critical values of x. In correspondence of these two values the free-energy density exhibits a discontinuity in its third derivative, and the log-gas experiences a third-order phase transition.

4.2. The void-band-void scenario (VBV). For large enough values of λ, and small enough values of $|\log x|$, we expect the particles to stay far away from the hard walls, and with relatively small density. In other words, we expect a single central band, $[a, b]$, between two voids, $[0, a]$ and $[b, \lambda]$. We shall denote such scenario by the acronym VBV. Calculations may be performed under the one-cut assumption.

4.2.1. *The resolvent.* We need to solve the saddle-point equation (3.7) where in the presently considered case the RHS reads

$$U(z) = V'(z) = 2\log z - 2\log(\lambda - z) + \log x.$$

Inserting into (3.8) and using the integration fomulae given in Appendix B, we obtain the following expression for the resolvent:

$$W(z) = \log\sqrt{x} + 2\log\frac{\sqrt{a(z-b)} + \sqrt{b(z-a)}}{\sqrt{(\lambda-a)(z-b)} + \sqrt{(\lambda-b)(z-a)}}. \tag{4.1}$$

Imposing the correct asymptotic behaviour provides the two equations

$$\frac{\sqrt{\lambda-a} + \sqrt{\lambda-b}}{\sqrt{a} + \sqrt{b}} = x^{1/4},$$

$$\lambda - \sqrt{ab} - \sqrt{\lambda-a}\sqrt{\lambda-b} = 1,$$

whose solution determines the end-points a and b, given by

$$a = \frac{(\sqrt{2\lambda-1} - x^{1/4})^2}{2(1+\sqrt{x})}, \qquad b = \frac{(\sqrt{2\lambda-1} + x^{1/4})^2}{2(1+\sqrt{x})}. \tag{4.2}$$

The corresponding equilibrium measure reads

$$\rho(z) = \frac{2}{\pi} \arctan \sqrt{\frac{(\lambda-a)(b-z)}{(\lambda-b)(z-a)}} - \frac{2}{\pi} \arctan \sqrt{\frac{a(b-z)}{b(z-a)}}, \quad z \in [a,b], \tag{4.3}$$

with a and b given by (4.2).

4.2.2. *The end-points of the band.* The present derivation and results are valid as long as the VBV scenario holds. A first condition for this is that the equilibrium measure (4.3), with a and b given by (4.2), satisfies the condition $\rho(z) < 1$. It is a simple calculation to verify that this indeed holds.

Also, the end-points (4.2) must satisfy the conditions $0 < a$ and $b < \lambda$. More precisely, we expect the VBV scenario to break down when $a = 0$, that is when $x = x_{\mathrm{c}}$, with

$$x_{\mathrm{c}} := (2\lambda - 1)^2, \tag{4.4}$$

or when $b = \lambda$, which occurs when $x = \tilde{x}_{\mathrm{c}}$, with $\tilde{x}_{\mathrm{c}} = (2\lambda-1)^{-2} \equiv x_{\mathrm{c}}^{-1}$. These two critical values separates three different regimes, labelled as follows. Regime I: $x > x_{\mathrm{c}}$, Regime II: $\tilde{x}_{\mathrm{c}} < x < x_{\mathrm{c}}$, and Regime III: $x < \tilde{x}_{\mathrm{c}}$, corresponding to the SBV, VBV, and VBS scenarios, respectively.

4.2.3. *The free-energy density.* We now turn to the evaluation of the free-energy density in the presently considered scenario, VBV, corresponding to values $x \in [\tilde{x}_{\mathrm{c}}, x_{\mathrm{c}}]$. Expanding the resolvent (4.1) to order z^{-2}, we get

$$E_{\mathrm{VBV}} = \frac{(a+b)(2\lambda-1) + \lambda(\sqrt{a}+\sqrt{b})^2}{4\sqrt{x}} \left(\frac{\sqrt{b}-\sqrt{a}}{\sqrt{b}+\sqrt{a}} \right)^2.$$

Replacing herein the expressions for the end-points (4.2), we get the first moment of the density:

$$E_{\mathrm{VBV}} = \frac{2\lambda-1}{2(1+\sqrt{x})} + \frac{1}{4},$$

which, recalling (3.9), implies

$$\begin{aligned}\Phi_{\mathrm{VBV}}(x) &= \frac{1}{4}\log x + (2\lambda-1)\log\frac{\sqrt{x}}{1+\sqrt{x}} + C \\ &= \frac{1}{4}\log x + (2\lambda-1)\log\frac{2\sqrt{x}}{1+\sqrt{x}} - \Psi(\lambda-1,\lambda-1),\end{aligned}$$

where the integration costant C has been determined by the condition $\Phi(1) = -\Psi(\lambda-1,\lambda-1)$, see (2.18) and (A.1). The free-energy density of the log-gas for $x \in [x_{\mathrm{c}}^{-1}, x_{\mathrm{c}}]$ may be equivalently written

$$\Phi_{\mathrm{VBV}}(x) = \left(\lambda - \frac{1}{4}\right)\log\frac{x}{x_{\mathrm{c}}} - (2\lambda-1)\log\frac{1+\sqrt{x}}{1+\sqrt{x_{\mathrm{c}}}} + \Phi_{\mathrm{c}}, \tag{4.5}$$

where

$$\Phi_{\mathrm{c}} := \Phi_{\mathrm{VBV}}(x_{\mathrm{c}}) = \frac{1}{2}\log x_{\mathrm{c}} - (\lambda-1)^2\log\frac{x_{\mathrm{c}}}{x_{\mathrm{c}}-1}, \tag{4.6}$$

is the value of free-energy density at the critical point.

4.3. The saturated-band-void scenario (SBV). We know that for values of x close to 1 the particles of the log-gas accumulate around the minimum of the potential, with a density that never saturates the constraint $\rho(u) = 1$. As we increase the value of x, the minimum of the potential moves to the left, and at some value x_{c} we may expect the left end-point of the support of the equilibrium measure to touch the left hard wall, with the emergence of a saturated interval for values $x > x_{\mathrm{c}}$, and hence, the transition to the SBV scenario.

4.3.1. *The resolvent.* The present scenario consists in a saturated interval $[0,a]$, a band $[a,b]$, and a void $[b,\lambda]$. In correspondence of the saturated interval $[0,a]$, where the equilibrium measure evaluates to one, the resolvent has a logarithmic cut with discontinuity $-2\pi\mathrm{i}$. This can be removed by introducing an auxiliary function $H(z)$ as follows,

$$W(z) = \log\frac{z}{z-a} + H(z).$$

Since $W(z)$ must solve (3.7), with $U(z) = V'(z)$, it follows that $H(z)$ must satisfy

$$H(z+\mathrm{i}0) + H(z-\mathrm{i}0) = \log x + 2\log\frac{z-a}{\lambda-z}, \qquad z \in [a,b].$$

The auxiliary resolvent $H(z)$ may now be evaluated in the standard way, using relation (3.8) and the identities of Appendix B. We finally get:

$$W(z) = \log\sqrt{x} + 2\log\frac{\sqrt{b-a}\sqrt{z}}{\sqrt{\lambda-a}\sqrt{z-b}+\sqrt{\lambda-b}\sqrt{z-a}}. \tag{4.7}$$

Requiring the asymptotic behaviour $W(z) \sim 1/z$, as $z \to \infty$, we obtain the two equations

$$\frac{\sqrt{\lambda-a}+\sqrt{\lambda-b}}{\sqrt{b-a}} = x^{1/4},$$
$$\lambda - \sqrt{\lambda-a}\sqrt{\lambda-b} = 1.$$

whose solution determines the end-points of the band. For $x > 1$, which is definitely holding in the presently considered case, namely $x > x_{\mathrm{c}}$, we have

$$a = \frac{\sqrt{x}+1-2\lambda}{\sqrt{x}-1},$$
$$b = \frac{\sqrt{x}-1+2\lambda}{\sqrt{x}+1}.$$

It is easily checked that the condition $a = 0$ reproduces the critical value $x_{\mathrm{c}} = (2\lambda-1)^2$.

The equilibrium measure reads

$$\rho(z) = \frac{2}{\pi}\arctan\sqrt{\frac{(\lambda-a)(b-z)}{(\lambda-b)(z-a)}}, \qquad z \in [a,b],$$

with $\rho(z) = 1$ for $z \in [0,a]$ and $\rho(z) = 0$ for $z > b$.

4.3.2. *The free-energy density.* Expanding the resolvent (4.7) to order z^{-2}, we get the first moment of the equilibrium measure

$$\begin{aligned} E_{\mathrm{SBV}} &= \frac{1}{4}\left[2\lambda(\lambda-\sqrt{\lambda-a}\sqrt{\lambda-b}) - (a+b)\sqrt{\lambda-a}\sqrt{\lambda-b}\right] \\ &= \frac{1}{2} + \frac{(\lambda-1)^2}{x-1}. \end{aligned}$$

Integrating, see (3.9), we obtain the free-energy density

$$\Phi_{\mathrm{SBV}}(x) = \frac{1}{2}\log x - (\lambda-1)^2\log\frac{x}{x-1}. \tag{4.8}$$

The condition (2.19) fixes the integration constant simply to zero. Note that the value $\Phi_{\mathrm{SBV}}(x_{\mathrm{c}})$ coincides with $\Phi_{\mathrm{c}} := \Phi_{\mathrm{VBV}}(x_{\mathrm{c}})$, reported in (4.6).

The function $\Phi(x)$ is thus continuous at $x = x_c$, as expected. It may be verified that the first and second derivatives of $\Phi(x)$ are continuous as well, over the whole interval $(\tilde{x}_c, \infty)$, while the third derivative is discontinuous at $x = x_c$. In other words, we observe the occurrence of a third-order phase transition in the free-energy density of the log-gas at $x = x_c$.

4.4. The void-band-saturated scenario (VBS). We now turn to values of the parameter x in the interval $x < \tilde{x}_c$. As seen above, when x tends to $\tilde{x}_c$ from above, the right end-point b of the band gets closer and closer to the hard wall located at $z = \lambda$. Decreasing the parameter x to values $x < \tilde{x}_c$, a saturated region arises to the right of the band, with the emergence of a VBS scenario.

4.4.1. *The resolvent.* In the presently considered scenario, consisting in a void $[0, a]$, a band $[a, b]$, and a saturated interval $[b, \lambda]$, the resolvent has a logarithmic cut in correspondence of the saturated interval, which can be removed by introducing an auxiliary function $H(z)$ as follows:

$$W(z) = \log \frac{z-b}{z-\lambda} + H(z).$$

This function must satisfy

$$H(z + \mathrm{i}0) + H(z - \mathrm{i}0) = \log x + 2 \log \frac{z}{b-z}, \qquad z \in [a, b].$$

The expression for the resolvent is therefore

$$W(z) = \log \sqrt{x} + 2 \log \frac{\sqrt{a}\sqrt{z-b} + \sqrt{b}\sqrt{z-a}}{\sqrt{b-a}\sqrt{z-\lambda}}, \tag{4.9}$$

yielding the equations for the end-points

$$\frac{\sqrt{b-a}}{\sqrt{a}+\sqrt{b}} = x^{1/4},$$
$$\lambda - \sqrt{ab} = 1,$$

whose solution is (for $x < 1$, which holds in the currently considered scenario):

$$a = \frac{1-\sqrt{x}}{1+\sqrt{x}}(\lambda - 1),$$
$$b = \frac{1+\sqrt{x}}{1-\sqrt{x}}(\lambda - 1).$$

It is easily checked that the condition $b = \lambda$ reproduces the critical value $\tilde{x}_{\mathrm{c}} = (2\lambda - 1)^{-2}$.

The equilibrium measure reads

$$\rho(z) = \frac{2}{\pi} \arctan \sqrt{\frac{b(z-a)}{a(b-z)}}, \qquad z \in [a, b].$$

with $\rho(z) = 0$ for $z \in [0, a]$ and $\rho(z) = 1$ for $z \in [b, \lambda]$. It is worth noting that all results worked out here for the VBS scenario can be obtained from those for the SBV scenario by means of the substitution $x \to x^{-1}$, $a \to \lambda - b$, and $b \to \lambda - a$.

4.4.2. *The free-energy density.* Expanding the resolvent (4.9) to order z^{-2}, we get

$$\begin{aligned} E_{\mathrm{VBS}} &= \frac{1}{4}\left[2\lambda^2 - (a+b)\sqrt{ab}\right] \\ &= \frac{\lambda^2}{2} - \frac{1}{2}(\lambda - 1)^2 \frac{1+x}{1-x}, \end{aligned}$$

which in turn implies:

$$\Phi_{\mathrm{VBS}}(x) = \frac{2\lambda - 1}{2} \log x + (\lambda - 1)^2 \log(1 - x). \tag{4.10}$$

The condition (2.21) fixes the integration constant simply to zero. It may be verified that the value $\Phi_{\mathrm{VBS}}(\tilde{x}_{\mathrm{c}})$ coincides with $\Phi_{\mathrm{VBV}}(\tilde{x}_{\mathrm{c}})$, and that the function $\Phi(x)$ is continuous at $x = \tilde{x}_{\mathrm{c}}$, as expected. It is just a matter of calculation to check that the first and second derivatives of $\Phi(x)$ are continuous as well, over the whole interval $(0, \infty)$, while the third derivative is discontinuous at $x = \tilde{x}_{\mathrm{c}}$.

Summing up, we have determined the free-energy density $\Phi(x)$ of the considered log-gas in the scaling limit, that is when $M - L = o(N)$ as $N \to \infty$. The expression of the free-energy density indicates that the system undergoes two third-order phase transitions, at $x = \tilde{x}_{\mathrm{c}}$ and $x = x_{\mathrm{c}}$, with $x_{\mathrm{c}} = (2\lambda - 1)^2 = \tilde{x}_{\mathrm{c}}^{-1}$.

5. The case $\lambda \neq \mu$

We now consider the same log-gas in a different scaling limit, namely when $M - L = O(N)$ as $N \to \infty$. Concerning the rescaled parameters, this implies $\lambda \neq \mu$. The situation appears to be significantly more complicated, with respect to the previous case, $\lambda = \mu$. As we shall see, four different

scenarios appear. They all have a single band $[a, b]$ (thus falling into the class of one-cut problems), between two gaps $[0, a]$ and $[b, \gamma]$, where $\gamma = \min(\lambda, \mu)$, which can be either voids or saturated regions.

Despite the presence of four different scenarios for the equilibrium measure of the log-gas, only two different phases, or regimes, will appear, with a single critical point. A similar situation was observed in [39], where a transition between two different scenarios could occur, with the free-energy density staying continuous together with all its derivatives, and hence without any phase transition, or change of regime.

5.1. Preliminaries. When $\lambda \neq \mu$, the potential of our log-gas is given by (3.3), with $z \in [0, \gamma]$, where $\gamma = \min(\lambda, \mu)$, with two hard walls at $z = 0$, and at $z = \gamma$.

The derivative of the potential reads:

$$V'(z) = 2\log z - \log(\lambda - z) - \log(\mu - z) + \log x. \tag{5.1}$$

Just as in the case $\mu = \lambda$, the derivative of the potential diverges in correspondence of the two hard walls, and the potential profile joins up smoothly to the hard walls on both sides. Letting $\lambda < \mu$ for definiteness, this is due to the terms "$\log z$" and "$\log(\lambda - z)$", in (5.1), for the left and right hard wall, respectively. Note however that now the coefficient of the term associated to the right hard wall is exactly 1. As we shall see below, this will imply, at variance with the symmetric case discussed in the previous Section, different behaviours in the free-energy density when, under variation of the parameters of the potential, the right end-point of the support of the equilibrium measure reaches the right hard wall.

The derivative of the potential vanishes at $z = z_\pm$, with

$$z_\pm := \frac{-(\lambda + \mu) \pm \sqrt{(\lambda + \mu)^2 + 4\lambda\mu(x - 1)}}{2(x - 1)}.$$

When $x > 1$, z_- is always negative, for any μ, λ. Vice versa, when $x < 1$, z_- is positive, but also always larger than γ. In both cases, only z_+ lies inside inside the interval $[0, \gamma]$, and actually strictly inside for any $x \in (0, \infty)$. It easy to verify that at $z = z_+$ the potential has a minimum.

Restricting to one-band scenarios, which will turn out to be sufficient for our purposes, the form of the potential suggests to investigate the four cases with a central band on the interval $[a, b]$, between two external intervals $[0, a]$, and $[b, \gamma]$, each of which may be saturated or void. Specifically we will discuss below the SBV, SBS, VBV, and VBS scenarios, in this order.

The potential being symmetric under interchange of the parameters λ and μ, we hereafter assume, with no loss of generality, that $\lambda < \mu$, and get rid of the parameter γ.

5.2. The saturated-band-void scenario (SBV). To start with, let us consider the case of relatively large x. The minimum of the potential, z_+, is then relatively close to the origin, and the particles tend to accumulate to the left. It is reasonable to expect an SBV scenario, with a saturated interval $[0, a]$, a band $[a, b]$ and a void $[b, \lambda]$.

5.2.1. *The resolvent and the band end-points.* Along with our usual procedure, we have

$$W(z) = \log \frac{z}{z-a} + H(z),$$

where the auxiliary resolvent $H(z)$ must now satisfy

$$H(z + \mathrm{i}0) + H(z - \mathrm{i}0) = V'(z) - 2 \log \frac{z}{z-a},$$

or, explicitly,

$$H(z + \mathrm{i}0) + H(z - \mathrm{i}0) = \log x + 2 \log(z-a) - \log(\mu - z) - \log(\lambda - z).$$

Standard calculations yield the following expression for the resolvent:

$$W(z) = \log \sqrt{x} + \log \frac{\sqrt{b-a}\sqrt{z}}{\sqrt{\lambda-a}\sqrt{z-b} + \sqrt{\lambda-b}\sqrt{z-a}} + \log \frac{\sqrt{b-a}\sqrt{z}}{\sqrt{\mu-a}\sqrt{z-b} + \sqrt{\mu-b}\sqrt{z-a}}. \quad (5.2)$$

Requiring the asymptotic behaviour $W(z) \sim 1/z$ as $z \to \infty$, we obtain the two equations

$$\frac{\sqrt{\mu-a} + \sqrt{\mu-b}}{\sqrt{\lambda-a} - \sqrt{\lambda-b}} = \sqrt{x}, \quad (5.3)$$

$$\mu + \lambda - \sqrt{\mu-a}\sqrt{\mu-b} - \sqrt{\lambda-a}\sqrt{\lambda-b} = 2. \quad (5.4)$$

Recalling that $\lambda < \mu$, it is evident from the first one that the currently considered scenario, SBV, may occur only for $x > 1$. The solution of these

two equations provides the end-points of the band,

$$a = \frac{x+1-\mu-\lambda-2\sqrt{x(\mu-1)(\lambda-1)}}{(x-1)}, \tag{5.5}$$

$$b = \frac{x+1-\mu-\lambda+2\sqrt{x(\mu-1)(\lambda-1)}}{(x-1)}. \tag{5.6}$$

where some simplifications have been done under the assumption $x > 1$, holding in the present scenario.

Clearly, the currently considered scenario, SBV, may hold only as long as $a \geqslant 0$, and $b \leqslant \lambda$. The first condition implies $x \geqslant x_{\rm c}$, where

$$x_{\rm c} := \left(\sqrt{\lambda\mu} + \sqrt{(\lambda-1)(\mu-1)}\right)^2. \tag{5.7}$$

It is easily checked that $x_{\rm c} > 1$. As for the second condition, it implies $x > x_1$, with

$$x_1 = \frac{\mu-1}{\lambda-1}. \tag{5.8}$$

It is easily checked that $x_1 > 1$, as well. Therefore the current scenario, SBV, holds for large x, down to the larger value between x_1 and $x_{\rm c}$, that is for $x > \max(x_1, x_{\rm c})$.

In the SBV scenario, the equilibrium measure reads

$$\rho(z) = \frac{1}{\pi}\arctan\sqrt{\frac{(\lambda-a)(b-z)}{(\lambda-b)(z-a)}} + \frac{1}{\pi}\arctan\sqrt{\frac{(\mu-a)(b-z)}{(\mu-b)(z-a)}}$$

for $z \in [a,b]$, with $\rho(z) = 1$ for $z \in [0,a]$, and $\rho(z) = 0$ for $z > b$.

5.2.2. *The free-energy density.* Expanding the resolvent (5.2) to order z^{-2}, we get

$$E_{\rm SBV} = \frac{1}{8}\Big[2\lambda(\lambda - \sqrt{\lambda-a}\sqrt{\lambda-b}) + 2\mu(\mu - \sqrt{\mu-a}\sqrt{\mu-b}) \\ - (a+b)\left(\sqrt{\lambda-a}\sqrt{\lambda-b} + \sqrt{\mu-a}\sqrt{\mu-b}\right)\Big].$$

This amounts to

$$E_{\rm SBV} = \frac{(\lambda-1)(\mu-1)}{x-1} + \frac{1}{2}, \qquad x > \max(x_1, x_{\rm c}), \tag{5.9}$$

which in turn implies the free-energy density

$$\Phi_{\rm SBV}(x) = \frac{1}{2}\log x - (\lambda-1)(\mu-1)\log\frac{x}{x-1}. \tag{5.10}$$

The condition (2.19) fixes the integration constant simply to zero.

5.3. The saturated-band-saturated scenario (SBS). When λ is relatively close to 1, and x tuned to have the minimum of the potential centered around $\lambda/2$, the SBS scenario may in principle occur. Let us investigate this possibility, with a band $[a, b]$ and two saturated intervals, $[0, a]$ and $[b, \lambda]$.

5.3.1. *The resolvent.* Following our standard procedure, we introduce an auxiliary resolvent $H(z)$, defined by

$$W(z) = \log \frac{z}{z-a} + \log \frac{z-b}{z-\lambda} + H(z),$$

and determined by the "potential"

$$V'(z) - 2\log \frac{z}{z-a} - 2\log \frac{b-z}{\lambda - z}, \qquad z \in [a, b].$$

Using the relations reported in Appendix B we obtain the following expression for the resolvent:

$$W(z) = \log \sqrt{x} + \log \frac{\sqrt{b-a}\sqrt{z}}{\sqrt{\lambda-a}\sqrt{z-b} - \sqrt{\lambda-b}\sqrt{z-a}} + \log \frac{\sqrt{b-a}\sqrt{z}}{\sqrt{\mu-a}\sqrt{z-b} + \sqrt{\mu-b}\sqrt{z-a}}. \quad (5.11)$$

Note that this expression for the resolvent may be formally obtained from that of the SBV scenario, Eq. (5.2), by means of the replacement $\sqrt{\lambda-b} \to -\sqrt{\lambda-b}$. Requiring the asymptotic behaviour $W(z) \sim 1/z$ as $z \to \infty$, we obtain the two equations

$$\frac{\sqrt{\mu-a} + \sqrt{\mu-b}}{\sqrt{\lambda-a} + \sqrt{\lambda-b}} = \sqrt{x},$$
$$\mu + \lambda - \sqrt{\mu-a}\sqrt{\mu-b} + \sqrt{\lambda-a}\sqrt{\lambda-b} = 2,$$

whose solution determines the position of the end-points a and b. Again note that these can be obtained from the corresponding equations (5.3) and (5.4) of the SBV scenario, by means of the replacement $\sqrt{\lambda-b} \to -\sqrt{\lambda-b}$. Note also that, since $\lambda < \mu$, it follows from the first equation that the present scenario may occur only for values of $x > 1$. Furthermore, comparison with (5.3) shows that it may occur for smaller values of x, with respect to the SBV scenario.

It appears that the solutions of these equations are given by (5.5) and (5.6), just as in the SBV scenario, provided that $x < x_1$. Clearly, decreasing the value of x, the SBV scenario will hold until x reaches the larger value between x_1 and x_c. If $x_1 > x_c$, the transition occurs at $x = x_1$, to the SBS scenario. If, instead, $x_1 < x_c$, the transition occurs at $x = x_c$, towards the VBV scenario. In other words, the SBS scenario may occur only if $x_1 > x_c$. In that event, it actually holds for all $x \in [x_c, x_1]$.

The requirement $x_1 > x_c$ selects the region

$$1 < \lambda < \frac{4}{3}, \qquad \mu > \frac{(2-\lambda)^2}{4-3\lambda}, \tag{5.12}$$

in the space of parameters $\mu > \lambda > 1$. In conclusion, the SBS scenario occurs if and only if the parameters λ and μ satisfy the condition (5.12). In this case the equilibrium measure reads

$$\rho(z) = 1 - \frac{1}{\pi} \arctan \sqrt{\frac{(\lambda-a)(b-z)}{(\lambda-b)(z-a)}} + \frac{1}{\pi} \arctan \sqrt{\frac{(\mu-a)(b-z)}{(\mu-b)(z-a)}}$$

for $z \in [a, b]$, with $\rho(z) = 1$ for $z \in [0, a] \cup [b, \lambda]$.

5.3.2. *The free-energy density.* Expanding the resolvent (5.11) to order z^{-2}, we get

$$E_{\mathrm{SBS}} = \frac{1}{8}\Big[2\lambda(\lambda + \sqrt{\lambda-a}\sqrt{\lambda-b}) + 2\mu(\mu - \sqrt{\mu-a}\sqrt{\mu-b}) \\ - (a+b)\left(\sqrt{\mu-a}\sqrt{\mu-b} - \sqrt{\lambda-a}\sqrt{\lambda-b}\right)\Big]$$

yielding

$$E_{\mathrm{SBS}} = \frac{(\lambda-1)(\mu-1)}{x-1} + \frac{1}{2}, \qquad x \in [x_c, x_1],$$

where the first expression could have as well been obtained from E_{SBV}, see (5.9) simply by means of the replacement $\sqrt{\lambda-b} \to -\sqrt{\lambda-b}$. As for the last expression, it evidently coincides with that for E_{SBV}, see the last line of (5.9). Integration yields the free-energy density,

$$\Phi_{\mathrm{SBS}}(x) = \frac{1}{2}\log x - (\lambda-1)(\mu-1)\log\frac{x}{x-1}, \tag{5.13}$$

whose expression evidently coincide with that in (5.10) for the SBV scenario. The integration constant has been fixed to zero by the sole requirement of continuity of the free-energy density at $x = x_1$.

In other words, the transition between the SBV and SBS scenarios (when present, that is only for $x_c < x_1$, or, equivalently, when λ and μ satisfy (5.12)), does not imply any phase transition in the model, the free-energy density being the same function on both sides of x_1. The same phenomenon had already been observed in [39]. In view of our considerations above, we denote both $\Phi_{\mathrm{SBV}}(x)$ and $\Phi_{\mathrm{SBS}}(x)$ by $\Phi_{\mathrm{I}}(x)$.

5.4. The void-band-void scenario (VBV). We recall that in the symmetric case, $\lambda = \mu$, for small values of $|\log x|$, the relevant scenario was VBV. It is reasonable to expect the same scenario holds for moderate differences between the values of λ and μ. Let us investigate this possibility, that is a band $[a, b]$, between two voids, $[0, a]$ and $[b, \lambda]$.

5.4.1. *The resolvent.* Inserting the derivative of the potential (5.1) into (3.8), and resorting to the integration formulae of Appendix B, we obtain the following expression for the resolvent:

$$W(z) = \log\sqrt{x} + \log\frac{\sqrt{a}\sqrt{z-b}+\sqrt{b}\sqrt{z-a}}{\sqrt{\lambda-a}\sqrt{z-b}+\sqrt{\lambda-b}\sqrt{z-a}} + \log\frac{\sqrt{a}\sqrt{z-b}+\sqrt{b}\sqrt{z-a}}{\sqrt{\mu-a}\sqrt{z-b}+\sqrt{\mu-b}\sqrt{z-a}}. \quad (5.14)$$

Requiring the asymptotic behaviour $W(z) \sim 1/z$ as $z \to \infty$, we obtain the two equations

$$\begin{aligned} &\frac{\left(\sqrt{\lambda-a}+\sqrt{\lambda-b}\right)\left(\sqrt{\mu-a}+\sqrt{\mu-b}\right)}{\left(\sqrt{a}+\sqrt{b}\right)^2} = \sqrt{x}, \\ &\lambda+\mu-\sqrt{\lambda-a}\sqrt{\lambda-b}-\sqrt{\mu-a}\sqrt{\mu-b} = 2+2\sqrt{a}\sqrt{b}, \end{aligned} \quad (5.15)$$

whose solution determines the position of the end-points a and b.

As we shall see below, the resolvent and the end-point equations are closely related to those of the VBS scenario, discussed in the next section. Just as for the SBV/SBS scenarios, the two scenarios VBV and VBS differ only in a change of sign of $\sqrt{\lambda-b}$, allowing for a unified treatment, see below. We also anticipate that, just as in the SBV/SBS transition, the transition between scenarios VBV and VBS does not imply a phase

transition. Before showing this, we report here, for completeness, the expression of the equilibrium measure in the VBV scenario:

$$\rho(z) = \frac{1}{\pi}\arctan\sqrt{\frac{(\lambda-a)(b-z)}{(\lambda-b)(z-a)}} + \frac{1}{\pi}\arctan\sqrt{\frac{(\mu-a)(b-z)}{(\mu-b)(z-a)}} - \frac{2}{\pi}\arctan\sqrt{\frac{a(b-z)}{b(z-a)}}, \qquad z\in[a,b],$$

with $\rho(z)=0$ for $z\in[0,a]\cup[b,\lambda]$.

5.5. The void-band-saturated scenario (VBS). We have seen above that in the symmetric case, for sufficiently small values of x, the relevant scenario is void-band-saturated. Let us investigate the consequences of such a scenario. We are thus considering the scenario with a void $[0,a]$, a band $[a,b]$ and a saturated interval $[b,\lambda]$. Recall that we assume $\lambda<\mu$.

5.5.1. *The resolvent.* We follow the standard procedure and introduce an auxiliary resolvent $H(z)$, such that

$$W(z) = \log\frac{z-b}{z-\lambda} + H(z),$$

determined by the auxiliary potential

$$U(z) = V'(z) - 2\log\frac{b-z}{\lambda-z}, \qquad z\in[a,b].$$

We obtain

$$W(z) = \log\sqrt{x} + \log\frac{\sqrt{a}\sqrt{z-b}+\sqrt{b}\sqrt{z-a}}{\sqrt{\lambda-a}\sqrt{z-b}-\sqrt{\lambda-b}\sqrt{z-a}} + \log\frac{\sqrt{a}\sqrt{z-b}+\sqrt{b}\sqrt{z-a}}{\sqrt{\mu-a}\sqrt{z-b}+\sqrt{\mu-b}\sqrt{z-a}}.$$

Imposing on the resolvent the asymptotic behaviour $W(z)\sim 1/z$, as $z\to\infty$, yields the two equations

$$\begin{aligned} \frac{\sqrt{b}-\sqrt{a}}{\sqrt{b}+\sqrt{a}}\,\frac{\sqrt{\mu-a}+\sqrt{\mu-b}}{\sqrt{\lambda-a}+\sqrt{\lambda-b}} &= \sqrt{x}, \\ \lambda+\mu+\sqrt{\lambda-a}\sqrt{\lambda-b}-\sqrt{\mu-a}\sqrt{\mu-b} &= 2+2\sqrt{ab}, \end{aligned} \tag{5.16}$$

whose solution determines the position of the end-points a and b.

Note that the resolvent $W(z)$ and the end-point equations are the same as in the VBV scenario, see (5.14) and (5.15), except for a change of sign $\sqrt{\lambda-b} \to -\sqrt{\lambda-b}$. We shall thus treat these two scenarios together below. Before this, let us report, for completeness, the expression for the equilibrium measure. We have

$$\rho(z) = \frac{1}{\pi}\arctan\sqrt{\frac{(\mu-a)(b-z)}{(\mu-b)(z-a)}} - \frac{1}{\pi}\arctan\sqrt{\frac{(\lambda-a)(b-z)}{(\lambda-b)(z-a)}} + \frac{2}{\pi}\arctan\sqrt{\frac{b(z-a)}{a(b-z)}}, \qquad z \in [a,b],$$

with $\rho(z) = 0$ for $z \in [0,a]$ and $\rho(z) = 1$ for $z \in [b,\lambda]$.

5.5.2. *The end-points.* We now turn to the solution of the end-point equations (5.15) and (5.16), for the VBV and VBS scenarios. As mentioned above, these equations differ just in a sign, and may be treated together. However, the derivation of their solution is a bit involved, and we report it in Appendix C. The resulting expression of the end-points, valid for both the VBV and the VBS scenarios, may be given in parametric form as follows:

$$a = A_+(t) + A_-(t) - 2\sqrt{A_+(t)A_-(t)}$$
$$b = A_+(t) + A_-(t) + 2\sqrt{A_+(t)A_-(t)}$$

where

$$A_+(t) = \frac{[(2\lambda-1)t+\lambda-\mu][(2\mu-1)t-\lambda+\mu]}{2t^2(\lambda+\mu+t)}$$
$$A_-(t) = \frac{(t+1)(t-\lambda+\mu)(t+\lambda-\mu)}{2t^2(\lambda+\mu+t)}$$

and t is determined by the value of x, as the unique root of

$$\frac{(1+t)^2(t-\lambda+\mu)(t+\lambda-\mu)}{[(2\lambda-1)t+\lambda-\mu][(2\mu-1)t-\lambda+\mu]} = x, \tag{5.17}$$

within the interval $[t_0,\infty)$, with $t_0 = \mu-\lambda > 0$.

To get some understanding of this result, and to prepare for the evaluation of the free-energy density, let us discuss some particular cases.

- In the limiting case $x \to 0^+$, the term "$z\log x$" in the potential (3.3) becomes the most relevant, and the particles tend to fully pack close to the hard wall at $z = \lambda$. In this limit the equilibrium

measure tends simply to a saturated interval $[\lambda-1,\lambda]$, while the band $[a,b]$ shrinks to zero, with both a and b tending to $\lambda-1$. This translates into $A_+=\lambda-1$, $A_-=0$, which occurs at $t_0:=\mu-\lambda$, corresponding, through (5.17), to $x=0$.

- It is easily verified that the value of $t\in[t_0,\infty)$ such that $x(t)=1$, with $x(t)$ defined by (5.17) is simply $t=\lambda+\mu-2$.
- The condition $a=0$ corresponds to the left end-point reaching the left hard wall, that is to the closure of the left gap $[0,a]$, and to its transition from void to saturated (i.e., to the transition between VBS and SBS scenarios). It translates here into $A_+=A_-$, which occurs at

$$t_{\rm c}=\Big(\sqrt{\lambda(\mu-1)}+\sqrt{(\lambda-1)\mu}\Big)^2,$$

which, using (5.17), yields

$$x_{\rm c}=\Big(\sqrt{\lambda\mu}+\sqrt{(\lambda-1)(\mu-1)}\Big)^2,$$

reproducing (5.7). Note the nice relation $t_{\rm c}=x_{\rm c}-1$.

- The condition $b=\lambda$ corresponds to the right end-point reaching the right hard wall, that is to the closure of the right gap $[b,\lambda]$, and to its transition from void to saturated (i.e., to the transition between VBS and VBV scenarios). This occurs when $B_+=B_-$, see Appendix C, that is at

$$t_2=\frac{(\lambda+1)(\mu-\lambda)+\sqrt{\lambda(\mu-\lambda)[(\lambda+4)\mu-(\lambda-2)^2]}}{2\lambda-1},$$

which, using (5.17), yields

$$\begin{aligned}x_2=\frac{1}{2(2\lambda-1)^3(\lambda+\mu-1)}\Big\{&-\lambda^4+2\lambda^3\mu-\lambda^2\mu^2\\&-10\lambda^3+10\lambda\mu^2+12\lambda^2-6\lambda\mu+2\mu^2-4\mu-4\lambda+2\\&+\big[(\lambda+4)\mu-(\lambda-2)^2\big]\sqrt{\lambda(\mu-\lambda)[(\lambda+4)\mu-(\lambda-2)^2]}\Big\}.\end{aligned}\tag{5.18}$$

This transition, as already commented, corresponds to a change of sign of $\sqrt{\lambda-b}$, which does not modify the analytic expression of the end-points, nor that of the free-energy density; as we shall see, it describes a change of scenario with no phase transition. Clearly, increasing the value of x, the VBS scenario will hold until x reaches the lowest value between x_2 and $x_{\rm c}$. If $x_2<x_{\rm c}$, the transition

occurs at $x = x_2$, to the VBV scenario. If, instead, $x_2 > x_c$, the transition occurs at $x = x_c$, towards the SBS scenario. In other words, the VBV scenario may occur only if $x_2 < x_c$. In that event it actually holds for all $x \in [x_2, x_c]$.

5.5.3. *The free-energy density.* We now turn to the evaluation of the free-energy density. We expand the resolvents (5.14) and (5.14) to order z^{-2}, obtaining

$$E = \frac{1}{8}\Big[-2(a+b)\sqrt{ab} + 2(\lambda^2+\mu^2) \\ -(a+b+2\mu)\sqrt{\mu-a}\sqrt{\mu-b} - \nu(a+b+2\lambda)\sqrt{\lambda-a}\sqrt{\lambda-b}\Big],$$

where $\nu = \pm 1$ for the VBV and VBS scenarios, respectively. Expressing E in terms of the quantities A's, B's, and C's defined in Appendix C, and using (C.11), we get

$$E = \frac{t^2+(8\lambda\mu-3\lambda-3\mu+2)t^2-3(\mu-\lambda)^2t+(\mu-\lambda)^2(\lambda+\mu-2)}{8t^2(\mu+\lambda+t)},$$

independently of the sign of ν, that is, of the scenario, VBV or VBS. Now, recalling that $E = x\partial_x\Phi(x)$, we have

$$\Phi(x(t)) = \int E\frac{\partial \log x}{\partial t}\mathrm{d}t + C,$$

where the function $x(t)$ follows from (5.17). Evaluating the integral for VBV and VBS scenarios, we find that $\Phi_{\mathrm{VBV}} = \Phi_{\mathrm{VBS}} =: \Phi_{\mathrm{II}}$, which reads

$$\Phi_{\mathrm{II}}(x(t)) = \frac{(\lambda+\mu-2)^2}{2}\log t + \frac{(\mu-\lambda)^2+2\lambda+2\mu-1}{2}\log(t+1) \\ + \frac{2\lambda-1}{2}\log(t+\lambda-\mu) + \frac{2\mu-1}{2}\log(t+\mu-\lambda) \\ -(\lambda+\mu-1)\log(t+\lambda+\mu) - \frac{2\lambda^2-2\lambda+1}{2}\log[(2\lambda-1)t+\lambda-\mu] \\ - \frac{2\mu^2-2\mu+1}{2}\log[(2\mu-1)t+\mu-\lambda] + C, \quad (5.19)$$

where

$$C = \frac{1}{2}\Big[(\lambda-1)^2\log 2(\lambda-1) + (\mu-1)^2\log 2(\mu-1) \\ + \lambda^2\log 2\lambda + \mu^2\log 2\mu\Big]$$

is the integration constant, fixed by imposing the initial condition $\Phi_{\rm II}(1) = -\Psi(\lambda-1,\mu-1)$, see (2.18) and (2.13), and recalling that $x(\lambda+\mu-2)=1$. Alternatively one may impose the initial condition (2.20), recalling that $x \to 0$ corresponds through (5.17) to $t \to t_0 = \mu - \lambda$. Expression (5.19) is valid for $t \in [\mu-\lambda, t_{\rm c}]$ (or $x \in [0, x_{\rm c}]$), independently of the value of t_2. When $t_2 > t_{\rm c}$ it just does not play any role. When $t_2 < t_{\rm c}$ (or $x_2 < x_{\rm c}$), at $t = t_2$ the transition between scenarios VBS and VBV occurs, with no effects on the free-energy density.

5.5.4. *The critical point $x_{\rm c}$ and the phase transition.* Summing up, we have evaluated the free-energy density of the log-gas in the case $\lambda \neq \mu$, with the following result. When $x > x_{\rm c}$, the free-energy density $\Phi_{\rm I}$ is given by (5.10), or equivalently, by (5.13). When $x < x_{\rm c}$, the free-energy density $\Phi_{\rm II}$ is given by (5.19).

To study the behaviour of the free-energy density in the vicinity of the critical point $x_{\rm c}$, it is convenient to employ the same parametrization for both $\Phi_{\rm I}$ and $\Phi_{\rm II}$, and thus to use parametrization (5.17), already used in $\Phi_{\rm II}$, for $\Phi_{\rm I}$ as well. We have

$$\begin{aligned}\Phi_{\rm I}(x(t)) &= 2(\lambda-1)(\mu-1)\log t - [2(\lambda-1)(\mu-1)-1]\log(t+1)\\ &- \frac{2\lambda\mu-2\lambda-2\mu+1}{2}\log(t+\lambda-\mu) - \frac{2\lambda\mu-2\lambda-2\mu+1}{2}\log(t+\mu-\lambda)\\ &+ (\lambda-1)(\mu-1)\log(t+\lambda+\mu) + (\lambda-1)(\mu-1)\log(t-\lambda-\mu+2)\\ &- \frac{1}{2}\log[(2\lambda-1)t+\lambda-\mu] - \frac{1}{2}\log[(2\mu-1)t+\mu-\lambda].\end{aligned}$$

It becomes now simply a matter of calculation to verify that both functions, together with their first and second derivatives, take the same value at $t = t_{\rm c}$, while their third derivatives take different values. In other words, the model undergoes a third-order phase transition at $x = x_{\rm c}$.

6. Discussion

We have evaluated the free-energy density $\Phi(x)$ of the log-gas described by (3.1) and (3.2). We want to discuss the obtained results, to compare them with previous works, and to explain their usefulness in relation to the study of phase separation phenomena in the five-vertex model.

6.1. Correspondence between scenarios and regimes. Two different scaling limits have been considered, namely the case $\lambda = \mu$, and the case $\lambda \neq \mu$, with quite different results. In the first case, as x is varied over

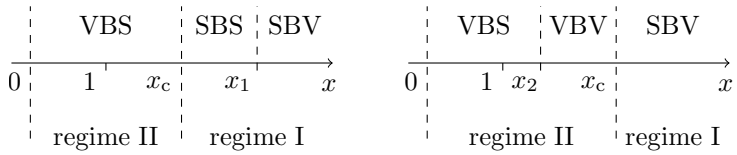

Fig. 3. Transitions betwen scenarios, and regimes, depending whether $x_1, x_2 > x_c$ (left) or $x_1, x_2 < x_c$ (right). Remarkably, despites very different expressions, for given values of λ and μ, x_1 and x_2 appears to be both smaller or both larger than x_c.

the range $x \in [0, \infty)$, there is a perfect correspondence between changes of scenarios and phase transitions: we have three possible scenarios, each one giving rise to a different expression for the free-energy density, and each change of scenario implies a discontinuity in the third derivative of the free-energy density, hence a third-order phase transition in the model.

In the second case, $\lambda \neq \mu$, the correspondence between scenarios and phases appears more complicated. Let us first state a few facts. When the potential has a hard wall at position $z = \alpha$, the contact between a band end-point and α implies a change of scenario, with a transition between void and saturated for the gap in the vicinity of α. Usually this change of scenario comes with a discontinuity in the third derivative of the free-energy density.

However, if (and only if) together with a hard wall at position $z = \alpha$, one has a term of the form $|z-\alpha| \log |z-\alpha|$ in the potential, *with coefficient 1*, the contact between a band end-point and α still implies a change of scenario, with a transition between void and saturated for the gap in the vicinity of α, but does not induce any singularity in the free-energy.

Therefore, when $\lambda = \mu$, and the coefficients of the terms $(\lambda - z)\log(\lambda - z)$ and $z \log z$ are both 2, the correspondence between changes of scenarios and phase transition is preserved. Conversely, when $\lambda \neq \mu$, the coefficient of the term $(\lambda - z)\log(\lambda - z)$, related to the hard wall at position λ becomes equal to 1, and the correspondence between changes of scenarios and phase transition is broken. More specifically, the left hard wall induces a phase transition together with the change of scenario, while the right does not.

In relation with these observation, it is worth mentioning the following fact. It is apparent from their expression, see (5.8) and (5.18), that $x_2 \neq x_1$. However, and remarkably, the two condition $x_1 > x_c$ and $x_2 > x_c$

coincide: they both select the region (5.12) in the space of parameters $\mu > \lambda > 1$. This is coherent with the fact that, for given values of λ and μ, the occurrence of the transition from SBV to SBS (requiring $x_1 > x_c$) is not compatible with that from VBS to VBV (requiring $x_2 < x_c$), see Fig. 3.

Indeed, for values of λ and μ satisfying (5.12), as x is decreased within the interval $[0, \infty)$, one has first the SBV scenario, corresponding to Regime I, till the value $x = x_1$ where the scenario changes to SBS, but not the regime (no singularity in the free-energy density), and next to the value $x = x_c$, where the scenario changes to VBS, with a third-order phase transition, to Regime II.

If instead the values of λ and μ do not satisfy (5.12), as x is decreased within the interval $[0, \infty)$, one has first the SBV scenario, corresponding to Regime I, till the value $x = x_c$ where the scenario changes to VBV, with a third-order phase transition, to Regime II, and, decreasing x further, at $x = x_2$ the scenario changes to VBS, still remaining in Regime II (no singularity in the free-energy density).

The interpretation provided above for the phases of the log-gas, in the two different scaling limits, and for their relations with the various scenarios for the equilibrium measure is complementary to that provided in [28], in a five-vertex model picture.

6.2. Comparison with previous results. We have evaluated the free-energy density $\Phi(x)$ of the log-gas described by (3.1) and (3.2). We want now to compare the obtained expressions with those worked out in [28], using a differential equation approach. To this aim recall that the free-energy density of the five-vertex model, $f_2(x)$, see (2.10), and that of the log-gas, $\Phi(x)$, see (2.16), are simply related by (2.17).

In the language of the five-vertex models, when the scaling limit is performed for an asymptotically square-shaped domain, $\lambda = \mu$, depending on the value of x, one has three regimes, labelled I, II, and III, and corresponding to the SBV, the VBV, and the VBS scenarios, respectively. These three regimes, or scenarios are separated by two critical points x_c, $\tilde{x}_c = x_c^{-1}$, with x_c given by (4.4). Inserting expressions (4.8), (4.5), and (4.10) into (2.17), one readily recover (upon replacement $\lambda \mapsto r + 1$) the expressions for $f_2^I(x)$, $f_2^{II}(x)$, and $f_2^{III}(x)$, respectively, as provided in [28, Theorem 1.1].

Similarly, when the scaling limit is performed for an asymptotically rectangular domain, $\lambda \neq \mu$, depending on the value of x, one has two

regimes, labelled I, II, separated by one critical point x_c given by (5.7). Inserting expressions (5.10), or equivalently (5.13), and (5.19) into (2.17), one readily recover (upon replacement $\lambda \mapsto p+1$ and $\mu \mapsto q+1$)) the expressions for $f_2^I(x)$ and $f_2^{II}(x)$, respectively, as provided in [28, Theorem 1.2].

6.3. Perspectives. Experience from the six-vertex model with domain-wall boundary conditions suggests the possibility of building a representation for some boundary correlation function of the five-vertex model in terms of the determinant of a matrix differing from the Hankel matrix appearing in (2.8) in just one column. As explained, e.g., in [33], for suitable forms of this modified column, it is then possible to relate such a determinantal representation to the log-gas model associated to (2.8). In particular, the asymptotic behaviour of such a boundary correlation function may be directly related to the resolvent of the log-gas.

Once the asymptotic behaviour of some boundary correlation function is explicitly evaluated, the phase separation curves of the model may be derived by using the "tangent method" [27]. In view of this the main result of the present paper is indeed the complete derivation of the free-energy of the five-vertex model within a log-gas description, and in particular the explicit expression for the resolvent in the various scenarios.

Appendix A. Asymptotic behaviour of MacMahon's formula

The number of boxed plane partitions is given by MacMahon formula (2.4). We want here to evaluate

$$\Psi(a,b) := \lim_{N\to\infty} \frac{1}{N^2} \log \mathrm{PL}(N, \lceil aN \rceil, \lceil bN \rceil).$$

Evaluating the limit we obtain

$$\Psi(a,b) = \int_0^1 [\ell(a+b+x) - \ell(a+x) - \ell(b+x) + \ell(x)]\, \mathrm{d}x,$$

where we have introduced the notation

$$\ell(x) := x \log x.$$

Standard calculations yields

$$\Psi(a,b) = \frac{1}{4}\Big[\ell\left(a^2\right) - \ell\left((a+1)^2\right) + \ell\left(b^2\right) - \ell\left((b+1)^2\right) \\ - \ell\left((a+b)^2\right) + \ell\left((a+b+1)^2\right)\Big],$$

In particular, we have

$$\Psi(0,b) = \Psi(a,0) = 0,$$
$$\Psi(a,a) = \frac{1}{2}(1+2a)^2\log(1+2a) - (1+a)^2\log(1+a) - a^2\log 4a.$$

For our purposes, in the main text it is convenient to rewrite the last expression in terms of $\lambda = a+1$. One has

$$\Psi\left(\lambda-1,\lambda-1\right) = \frac{(2\lambda-1)^2}{2}\log(2\lambda-1) - \lambda^2\log\lambda \\ - (\lambda-1)^2\log(\lambda-1) - 2(\lambda-1)^2\log 2. \quad \text{(A.1)}$$

Appendix B. Useful integrals

Let us recall a few identities, which turn useful in the evaluation of the resolvent. The first, obvious one, is simply

$$\int_a^b \frac{1}{(z-u)\sqrt{(u-a)(b-u)}}\,\mathrm{d}u = \frac{\pi}{\sqrt{(z-a)(z-b)}}, \qquad z\in\mathbb{C}\backslash[a,b],$$

We also have

$$\int_a^b \frac{1}{(z-u)\sqrt{(u-a)(b-u)}}\log\frac{u-c}{u-d}\,\mathrm{d}u$$
$$= \begin{cases} \dfrac{2\pi}{\sqrt{(z-a)(z-b)}}\log\dfrac{\sqrt{a-c}\sqrt{z-b}+\sqrt{b-c}\sqrt{z-a}}{\sqrt{a-d}\sqrt{z-b}+\sqrt{b-d}\sqrt{z-a}}, & c,d\leqslant a, \\ \dfrac{2\pi}{\sqrt{(z-a)(z-b)}}\log\dfrac{\sqrt{c-a}\sqrt{z-b}+\sqrt{c-b}\sqrt{z-a}}{\sqrt{d-a}\sqrt{z-b}+\sqrt{d-b}\sqrt{z-a}}, & c,d\geqslant b, \end{cases}$$

and

$$\int_a^b \frac{1}{(z-u)\sqrt{(u-a)(b-u)}} \log\frac{u-c}{d-u}\,\mathrm{d}u$$
$$= \frac{2\pi}{\sqrt{(z-a)(z-b)}} \log\frac{\sqrt{a-c}\sqrt{z-b}+\sqrt{b-c}\sqrt{z-a}}{\sqrt{d-a}\sqrt{z-b}+\sqrt{d-b}\sqrt{z-a}}, \qquad c \leqslant a, b \leqslant d,$$

which all hold for $z \in \mathbb{C}\backslash[a,b]$.

Finally, we report a useful identity to evaluate the equilibrium measure from the expression of the resolvent. Let

$$f(z) = \log\left[\sqrt{\alpha(z-a)}+\sqrt{\beta(z-b)}\right],$$

then

$$f(x+\mathrm{i}0) - f(x+\mathrm{i}0) = 2\mathrm{i}\arctan\sqrt{\frac{\beta(b-x)}{\alpha(x-a)}}, \qquad z \in [a,b].$$

Appendix C. The solution of the end-point equations (5.15) and (5.16)

We report here the solution of the end-point equations (5.15) and (5.16), for the VBV and VBS scenarios. We follow an approach proposed in [39], for a similar problem.

As mentioned these equations differ just in a sign, and may be treated together. To start with, let us rewrite the two sets of end-point equations in a unified way:

$$\begin{aligned} \frac{\sqrt{b}-\sqrt{a}}{\sqrt{b}+\sqrt{a}}\frac{\sqrt{\mu-a}+\sqrt{\mu-b}}{\sqrt{\lambda-a}-\nu\sqrt{\lambda-b}} &= \sqrt{x}, \\ \lambda+\mu-\nu\sqrt{\lambda-a}\sqrt{\lambda-b}-\sqrt{\mu-a}\sqrt{\mu-b} &= 2+2\sqrt{ab}, \end{aligned} \tag{C.1}$$

where

$$\nu = \begin{cases} +1 & \text{for scenario VBV,} \\ -1 & \text{for scenario VBS.} \end{cases}$$

Note that, from the form of the first equation it follows that the values $\nu = -1$, that is the VBS scenario, corresponds to lower values of x.

Instead of dealing with the end-points a and b as unknowns, we introduce the quantities

$$\begin{aligned} A_\pm &= \frac{1}{4}\left(\sqrt{b} \pm \sqrt{a}\right)^2, \\ B_\pm &= \frac{1}{4}\left(\sqrt{\lambda - a} \pm \nu\sqrt{\lambda - b}\right)^2, \\ C_\pm &= \frac{1}{4}\left(\sqrt{\mu - a} \pm \sqrt{\mu - b}\right)^2. \end{aligned}$$

Clearly, the end-points may be expressed in terms of these new quantities, e.g.,

$$a = A_+ + A_- - 2\sqrt{A_+A_-}, \qquad b = A_+ + A_- + 2\sqrt{A_+A_-},$$

and similarly in terms of B's or C's. These quantities also satisfy some consistency relations, of multiplicative,

$$A_+A_- = B_+B_- = C_+C_-, \tag{C.2}$$

or additive form

$$A_+ + A_- = \lambda - B_+ - B_- = \mu - C_+ - C_-. \tag{C.3}$$

The first equation in (C.1) reads now

$$\frac{A_-C_+}{A_+B_-} = x, \tag{C.4}$$

and the second one can be written in either of the two forms

$$2A_\pm + B_\pm + C_\pm = N_\pm, \tag{C.5}$$

where

$$N_+ := \lambda + \mu - 1, \qquad N_- := 1.$$

Clearly, (C.2)–(C.5) constitute a system of six equations in the six unknowns $A_\pm$, $B_\pm$, and $C_\pm$. Also, the equivalence of two forms of (C.5) is easily checked, just rewriting (C.3) as

$$\begin{aligned} A_+ + A_- + B_+ + B_- &= \lambda, \\ A_+ + A_- + C_+ + C_- &= \mu, \end{aligned} \tag{C.6}$$

and summing the two equations.

Let us now turn to the solution of this system of equations. Dividing the two equations in (C.5) by $\sqrt{B_\pm C_\pm}$, respectively, and using the relation

$B_+/C_+ = C_-/B_-$, see (C.2), comparison of the resulting relations yields

$$\frac{N_+ - 2A_+}{\sqrt{B_+C_+}} = \frac{N_- - 2A_-}{\sqrt{B_-C_-}}.$$

From the ratio of these two relations, and (C.2), we may now express the B's in terms of the A's and C's, as follows

$$C_\pm = B_\mp \frac{w_\pm}{w_\mp}, \tag{C.7}$$

where we have used the notation

$$w_\pm := N_\pm - 2A_\pm. \tag{C.8}$$

We may now use these relations into (C.6), to eliminate the C's, and to express the A's in terms of the w's; we get

$$\begin{aligned} B_+ + B_- &= \frac{w_+ + w_-}{2} - \frac{\mu - \lambda}{2}, \\ B_+ \frac{w_-}{w_+} + B_- \frac{w_+}{w_-} &= \frac{w_+ + w_-}{2} + \frac{\mu - \lambda}{2}, \end{aligned}$$

and solving for the B's,

$$B_\pm = \left(1 \mp \frac{\mu - \lambda}{w_+ - w_-}\right) \frac{w_\pm}{2}. \tag{C.9}$$

Recalling that $B_+B_- = A_+A_-$, see (C.2), we have

$$\left[1 - \frac{(\mu - \lambda)^2}{(w_+ - w_-)^2}\right] w_+w_- = (N_+ - w_+)(N_- - w_-),$$

which turns into a cubic equation for the w's

$$(\mu - \lambda)^2 w_+w_- = (N_+w_- + N_-w_+ - N_+N_-)\,(w_+ - w_-)^2.$$

Note that it contains only terms of degree two and three, thus describing a rational curve. This means the w's can be expressed as rational functions of some parameter along the curve.

To obtain this parametrization, we set $w_+ = (t+1)w_-$, and consider w_- as a funtion of the parameter t; we have

$$\begin{aligned} w_+ &= (t+1)w_-, \\ w_- &= \frac{1}{N_+ + N_-(t+1)} \left[N_+N_- + (\mu - \lambda)^2 \frac{(t+1)}{t^2}\right]. \end{aligned} \tag{C.10}$$

Note that we need just the portion of the curve corresponding to the regime of interest. As we shall see below, this is given by $t \in [t_0, \infty)$, with $t_0 := \mu - \lambda > 0$.

Substituting now (C.10) into (C.7), (C.8), and (C.9), we finally obtain

$$\begin{aligned}
A_+ &= \frac{[(2\lambda-1)t+\lambda-\mu][(2\mu-1)t-\lambda+\mu]}{2t^2(\lambda+\mu+t)},\\
A_- &= \frac{(t+1)(t-\lambda+\mu)(t+\lambda-\mu)}{2t^2(\lambda+\mu+t)},\\
B_+ &= \frac{(t+1)(t+\lambda-\mu)[(2\lambda-1)t+\lambda-\mu]}{2t^2(\lambda+\mu+t)},\\
B_- &= \frac{(t-\lambda+\mu)[(2\mu-1)t-\lambda+\mu]}{2t^2(\lambda+\mu+t)},\\
C_+ &= \frac{(t+1)(t-\lambda+\mu)[(2\mu-1)t-\lambda+\mu]}{2t^2(\lambda+\mu+t)},\\
C_- &= \frac{(t+\lambda-\mu)[(2\lambda-1)t+\lambda-\mu]}{2t^2(\lambda+\mu+t)}.
\end{aligned} \tag{C.11}$$

These expressions for the A's, B's, and C's solve equations (C.2), (C.3), and (C.5). It can be checked that they are all positive, as long as $t \in [t_0, \infty]$.

Note that we have not used equation (C.4), yet. To obtain the solution for the end-points we need to fix $t \in [t_0, \infty)$. This is done indeed by means of (C.4), which using (C.11) yields precisely (5.17). This is a quartic equation, with in principle four different roots for any given value of x. It may be verified that for any given $x > 0$, there is one and only one real root in $[t_0, \infty)$, and that, as t varies over this interval, x increases monotonously, spanning the whole interval $[0, \infty)$.

Acknowledgments

We are indebted to Nikolai M. Bogoliubov, Andrea Maroncelli, and Matteo Mucciconi for stimulating discussions.

References

1. R. J. Baxter, *Exactly solved models in statistical mechanics*, Academic Press, San Diego, CA, 1982.
2. C. Garrod, A. C. Levi, and M. Touzani, *Mapping of crystal growth onto the 6-vertex model*, — Solid State Commun. **75** (1990), 375–382.

3. C. Garrod, *Stochastic models of crystal growth in two dimensions*, — Phys. Rev. A **41** (1990), 4184–4194.
4. M. Gulácsi, H. van Beijeren, and A.C. Levi, *Phase diagram of the five-vertex model*, — Phys. Rev. E **47** (1993), 2473–2483.
5. J. D. Noh and D. Kim, *Interacting domain walls and the five-vertex model*, — Phys. Rev. E **49** (1994), 1943–1961.
6. H.Y. Huang, F.Y. Wu, H. Kunz, and D. Kim, *Interacting dimers on the honeycomb lattice: an exact solution of the five-vertex model*, — Physica A **47** (1996), 1–32.
7. K. Motegi and K Sakai, *Vertex models, TASEP and Grothendieck polynomials*, — J. Phys. A **46** (2013), 355201.
8. K. Motegi and K. Sakai, *K-theoretic boson-fermion correspondence and melting crystals*, — J. Phys. A **47** (2014), 445202.
9. B. Brubaker, V. Buciumas, D. Bump, and H. P. A. Gustafsson, *Colored five-vertex models and Demazure atoms*, — J. Combin. Theory A **178** (2021), 105354.
10. K. Motegi, *Integrability approach to Fehér-Némethi-Rimányi-Guo-Sun type identities for factorial Grothendieck polynomials*, — Nucl. Phys. B **954** (2020), 114998.
11. J. de Gier, R. Kenyon, and S. Watson, *Limit shapes for the asymmetric five vertex model*, — Commun. Math. Phys. **385** (2021), 793–836.
12. R. Kenyon and I. Prause, *The genus-zero five vertex model*, — Prob. Math. Phys. **3** (2022), 707–729.
13. R. Kenyon and I. Prause, *Gradient variational problem in* $\mathbb{R}^2$, — Duke Math. J. **171** (2022), 3003–3022.
14. R. Kenyon and I. Prause, *Limit shapes from harmonicity: dominos and the five vertex model*, — J. Phys. A: Math. Theor. **57** (2024), 035001.
15. V. E. Korepin, N. M. Bogoliubov, and A. G. Izergin, *Quantum Inverse Scattering Method and Correlation Functions*, Cambridge University Press, Cambridge, 1993.
16. N. M. Bogoliubov, *Four-vertex model and random tilings*, — Theor. Math. Phys. **155** (2008), 523–535.
17. N. M. Bogoliubov, *Five-vertex model with fixed boundary conditions*, — St. Peterburg Math. J. **21** (2010), 407–421.
18. N. M. Bogolyubov and C. L. Malyshev, *Integrable models and combinatorics*, — Russian Math. Surveys **70** (2015), 789–856.
19. N. M. Bogoliubov and A. G. Pronko, *One-point function of the four-vertex model*, — J. Math. Sci. **275** (2023), 249–258.
20. N. M. Bogoliubov and C. L. Malyshev, *Scalar product of the five-vertex model and complete symmetric polynomials*, — J. Math. Sci. **284** (2024), 654–664.
21. A. G. Pronko, *The five-vertex model and enumerations of plane partitions.* — J. Math. Sci. **213** (2016), 756–768.
22. I. N. Burenev and A. G. Pronko, *Determinant formulas for the five-vertex model*, — J. Phys. A: Math. Theor. **54** (2021), 055008.
23. A. Maroncelli, *Limit shape phenomena in statistical mechanics*, 2024, PhD thesis, University of Florence (unpublished).
24. V. E. Korepin, *Calculations of norms of Bethe wave functions*, — Commun. Math. Phys. **86** (1982), 391–418.

25. A. G. Izergin, *Partition function of the six-vertex model in the finite volume*, — Sov. Phys. Dokl. **32** (1987), 878–879.
26. N. M. Bogoliubov, A. G. Pronko, and M. B. Zvonarev, *Boundary correlation functions of the six-vertex model*, — J. Phys. A **35** (2002), 5525–5541.
27. F. Colomo and A. Sportiello, *Arctic curves of the six-vertex model on generic domains: The tangent method*, — J. Stat. Phys. **164** (2016), 1488–1523.
28. I. N. Burenev and A. G. Pronko, *Thermodynamics of the five-vertex model with scalar-product boundary conditions*, — Commun. Math. Phys. **405** (2024), 148.
29. A.V. Kitaev and A.G.Pronko, *Emptiness formation probability of the six-vertex model and the sixth Painlevé equation*, — Commun. Math. Phys. **345** (2016), 305–354.
30. M. Jimbo and T. Miwa, *Monodromy preserving deformation of linear ordinary differential equations with rational coefficients. II*, — Physica D **2** (1981), 407–448.
31. K. Okamoto, *Studies on the Painlevé equations. I: sixth Painlevé equation P_{VI}*, — Ann. Mat. Pura Appl. **146** (1987), 337–381.
32. P. Zinn-Justin, *Six-vertex model with domain wall boundary conditions and one-matrix model*, — Phys. Rev. E **62** (2000), 3411–3418.
33. F. Colomo, A. G. Pronko, and P. Zinn-Justin, *The arctic curve of the domain-wall six-vertex model in its anti-ferroelectric regime*, — J. Stat. Mech. Theory Exp. (2010), L03002.
34. P.J. Forrester, *Log-gases and random matrices*, London Mathematical Society Monographs, vol. 34, Princeton University Press, Princeton, NJ, 2010.
35. I. N. Burenev, F. Colomo, A. Maroncelli, and A. G. Pronko, *Arctic curves of the four-vertex model*, — J. Phys. A: Math. Theor. **55** (2023), 465202.
36. J. Baik, T. Kriecherbauer, K. T.-R. McLaughlin, and P. D. Miller, *Discrete orthogonal polinomials: Asymptotics and applications*, Ann. of Math. Stud., vol. 164, Princeton University Press, Princeton, NJ, 2007.
37. M. R. Douglas and V. A. Kazakov, *Large N phase transition in continuum QCD_2*, — Phys. Lett. B **319** (1993), 219–230.
38. P. D. Dragnev and E. B. Saff., *A problem in potential theory and zero asymptotics of Krawtchouk polynomials*, — J. Approx. Theory **102** (2000), 120–140.
39. F. Colomo and A. G. Pronko, *Thermodynamics of the six-vertex model in an L-shaped domain*, — Comm. Math. Phys. **339** (2015), 699–728.

Поступило 10 ноября 2025 г.

INFN, Sezione di Firenze
Via G. Sansone 1, 50019 Sesto Fiorentino (FI), Italy
E-mail: colomo@fi.infn.it

Dipartimento di Fisica e Astronomia, Università di Firenze
Via G. Sansone 1, 50019 Sesto Fiorentino (FI), Italy
E-mail: michelangelo.mannatzu@gmail.com

St. Petersburg Department of V. A. Steklov
Mathematical Institute,
Fontanka 27, 191023 St. Petersburg, Russia
E-mail: a.g.pronko@gmail.com